



Implementation of DNA Methylation Array Profiling in Pediatric Central Nervous System

Q1 Q10 Tumors

Q2 The AIM BRAIN Project: An Australian and New Zealand Children's Hematology and Oncology Group Study

Q51 Christine L. White,^{*†‡} Kathryn M. Kinross,^{*†§} Molly K. Buntine,^{*†} Elnaz Rasouli,^{*†} Robyn Strong,^{*†§} Janelle M. Jones,^{*†§} Jason E. Cain,^{*†} Dominik Sturm,^{¶||**} Felix Sahm,^{¶††††} David T.W. Jones,^{¶||} Stefan M. Pfister,^{¶**§§} Thomas Robertson,^{¶¶} Colleen D'Arcy,^{¶|||} Michael L. Rodriguez,^{***} Jason M. Dyke,^{†††††} Reimar Junckerstorff,^{†††††} Dharmesh D. Bhuva,^{§§§¶¶¶} Melissa J. Davis,^{§§§¶¶¶} Paul Wood,^{¶||||} Tim Hassall,^{****} David S. Ziegler,^{††††††§§§§} Stewart Kellie,^{¶¶¶¶} Geoffrey McCowage,^{¶¶¶¶} Frank Alvaro,^{¶|||||} Maria Kirby,^{*****} John A. Heath,^{†††††} Karen Tsui,^{†††††} Andrew Dodgshun,^{§§§§§} David D. Eisenstat,^{¶¶¶¶¶|||} Dong-Anh Khuong-Quang,^{¶¶¶¶¶} Meaghan Wall,[‡] Elizabeth M. Algar,^{*†} Nicholas G. Gottardo,^{*****†††††} and Jordan R. Hansford,^{¶¶¶¶¶***¶¶¶¶¶|||†††††}

Q3 Q4 From the Hudson Institute of Medical Research,* Clayton, Victoria, Australia; the Department of Molecular and Translational Science,[†] Monash University, Clayton, Victoria, Australia; the Victorian Clinical Genetics Services,[‡] Parkville, Victoria, Australia; the Australian and New Zealand Children's Haematology/Oncology Group,[§] Clayton, Victoria, Australia; the Hopp Children's Cancer Centre Heidelberg,[¶] Heidelberg, Germany; the Divisions of Pediatric Glioma Research^{||} and Pediatric Neurooncology^{§§} and the Clinical Cooperation Unit Neuropathology,^{††} German Cancer Research Center and German Cancer Consortium, Heidelberg, Germany; the Departments of Pediatric Oncology, Hematology and Immunology^{**} and Neuropathology,^{††} Heidelberg University Hospital, Heidelberg, Germany; the Royal Brisbane and Women's Hospital,^{¶¶} Herston, Queensland, Australia; the Department of Pathology,^{|||} Royal Children's Hospital, Parkville, Victoria, Australia; the Sydney Children's Hospital,^{***} Randwick, New South Wales, Australia; PathWest Neuropathology,^{†††} Royal Perth Hospital, Perth, Western Australia, Australia; Pathology and Laboratory Medicine,^{†††} University of Western Australia, Nedlands, Western Australia, Australia; the Walter and Eliza Hall Institute,^{§§§} Melbourne, Victoria, Australia; the South Australia ImmunoGENomics Cancer Institute,^{¶¶¶} University of Adelaide, Adelaide, South Australia, Australia; the Monash Children's Hospital,^{¶¶¶} Clayton, Victoria, Australia; the Queensland Children's Hospital,^{****} South Brisbane, Queensland, Australia; the Kids Cancer Centre,^{††††} Sydney Children's Hospital, Randwick, New South Wales, Australia; the Children's Cancer Institute,^{††††} Lowy Cancer Research Centre, UNSW, Kensington, New South Wales, Australia; the School of Clinical Medicine,^{§§§§} UNSW Medicine and Health, UNSW Sydney, Sydney, New South Wales, Australia; The Children's Hospital at Westmead,^{¶¶¶¶} Westmead, New South Wales, Australia; the John Hunter Children's Hospital,^{¶¶¶¶¶} New Lambton Heights, New South Wales, Australia; the Women's and Children's Hospital,^{*****} North Adelaide, South Australia, Australia; the Royal Hobart Hospital,^{†††††} Hobart, Tasmania, Australia; the Starship Children's Hospital,^{†††††} Grafton, Auckland, New Zealand; the Christchurch Hospital,^{§§§§§} Christchurch Central City, Christchurch, New Zealand; the Children's Cancer Centre,^{¶¶¶¶¶} Royal Children's Hospital, Parkville, Victoria, Australia; the Murdoch Children's Research Institute,^{¶¶¶¶¶} Department of Paediatrics, University of Melbourne, Melbourne, Victoria, Australia; the Perth Children's Hospital,^{*****} Nedlands, Western Australia, Australia; the Telethon Kids Institute,^{†††††} Nedlands, Western Australia, Australia; and the South Australia Health and Medical Research Institute,^{†††††} Adelaide, South Australia, Australia

Accepted for publication
June 7, 2023.

Address correspondence to
Elizabeth M. Algar, Hudson
Institute of Medical Research,
21–31 Wright St., Clayton,
VIC, 3168 Australia.
E-mail: elizabeth.algar@monash.edu.au

DNA methylation array profiling for classifying pediatric central nervous system (CNS) tumors is a valuable adjunct to histopathology. However, unbiased prospective and interlaboratory validation studies have been lacking. The AIM BRAIN diagnostic trial involving 11 pediatric cancer centers in Australia and New Zealand was designed to test the feasibility of routine clinical testing and ran in parallel with the Molecular Neuropathology 2.0 (MNP2.0) study at Deutsches Krebsforschungszentrum (German Cancer Research Center). CNS tumors from 269 pediatric patients were prospectively tested on Illumina EPIC arrays, including 104 cases co-enrolled on MNP2.0. Using MNP classifier versions 11b4 and 12.5, we report classifications with a probability score ≥ 0.90 in 176 of 265 (66.4%) and 213 of 269 (79.2%) cases, respectively. Significant diagnostic information was obtained in 130 of 176 (74%) for

11b4, and 12 of 174 (7%) classifications were discordant with histopathology. Cases prospectively co-enrolled on MNP2.0 gave concordant classifications (99%) and score thresholds (93%), demonstrating excellent test reproducibility and sensitivity. Overall, DNA methylation profiling is a robust single workflow technique with an acceptable diagnostic yield that is considerably enhanced by the extensive subgroup and copy number profile information generated by the platform. The platform has excellent test reproducibility and sensitivity and contributes significantly to CNS tumor diagnosis. (*J Mol Diagn* 2023, ■: 1–20; <https://doi.org/10.1016/j.jmoldx.2023.06.013>)

In the past decade, significant advances have been made in the classification of brain tumors in both children and adults. Traditionally, diagnosis was based solely on the tumor's histopathology, cellular architecture, anatomic location, and clinical presentation. Twenty years ago, molecular and cytogenetic biomarkers emerged as potential additional diagnostic tools, enabling specific central nervous system (CNS) tumor types to be more precisely classified and grouped according to likely clinical outcome based on response to chemotherapy, radiotherapy, and molecular targeted therapies. In 2016, the World Health Organization (WHO) included many of these recognized molecular markers into the classification system, to provide an integrated diagnosis combining histopathology and molecular biomarkers.^{1,2} Notably, this was expanded on in the most recent fifth edition (2021) and now includes DNA methylation profiling as an important adjunct to conventional histopathology for tumors in the CNS.^{3,4}

DNA methylation profiling is a powerful objective technique for classifying CNS tumors with capacity to distinguish >80 CNS tumor groups and subgroups.^{5,6} Capper et al⁵ pioneered methylome analysis and showed that distinct tumor types could be described by applying a random forest algorithm with multinomial logistic regression to methylation data derived from tumors with comprehensive prior histologic and molecular characterizations. The platform was developed and prospectively tested at Deutsches Krebsforschungszentrum (DKFZ; German Cancer Research Center, Heidelberg, Germany) in a large series of pediatric and adult CNS tumors, culminating in the development of an online tumor classification tool that is currently freely available.⁶ Tumor classifications are derived by uploading raw DNA methylation data from Illumina (San Diego, CA) EPIC methylation arrays to the online platform. Classifier iterations are updated as new tumor types are described. The range of reference CNS tumor classes is listed online (<https://www.molecularneuropathology.org/mnp/classifiers>, last accessed May 29, 2023). Further independent studies followed, describing the utility and

limitations of methylome analysis for classifying CNS tumors.^{7–10} Data from array-based methylome analysis also provide additional information on tumor chromosomal abnormalities, potentially reducing the need for molecular cytogenetics.

Here, we report on findings from the first 3.5 years of the AIM BRAIN (AB) project (Access to Innovative Molecular Diagnostic Profiling in Brain Tumors), a prospective diagnostic clinical trial testing DNA methylation profiling for the classification of CNS tumors in children and young adults in Australia and New Zealand. We extend previous studies by presenting the results of interlaboratory comparative testing on 104 cases to assess reproducibility and to establish parameters for test sensitivity and specificity. We report optimal thresholds for tumor content, array data quality, and test utility as a prelude to implementing tumor methylome analysis as a routine nationally accredited clinical test within an Australian pathology service.

Materials and Methods

Ethics, Eligibility, and Data Collection

AB was sponsored by the cooperative research group Australian and New Zealand Children's Hematology/Oncology Group. All 11 public hospital pediatric cancer centers throughout Australia and New Zealand were participating sites. Ethical approval was obtained from The Royal Children's Hospital Human Research Ethics Committee (reference number 17/RCHM/306), Tasmania Human Research Ethics Committee (reference number 20523), and New Zealand Central Health and Disability Ethics Committee (reference number 19/CEN/16). Participants were eligible if they had a suspected or confirmed primary brain or spinal cord tumor (at diagnosis or relapse); had an adequate sample; and were aged ≤ 21 years.

Patient selection was at the discretion of site treating teams and not known to the National Coordinating Center for the study. All participants and/or their parents or legal guardians must have signed a written informed consent.

Patient data and test results were maintained in a REDCap database with access granted only to authorized clinical and laboratory researchers. Patient data collected from the participating sites included age, sex, demographics, treatment and medical history, pathology information, follow-up, and site investigator's impact statement.

Supported by Cancer Australia, the Robert Connor Dawes Foundation, and Carrie's Beans 4 Brain Cancer Foundation. Institutional support provided through the Victorian Government's Operational Infrastructure Support Program.

Disclosures: None declared.

E.M.A., N.G.G., and J.R.H. were the study principal investigators and contributed equally to this work.

Specimens

DNA methylation profiling was performed in the laboratory located at Monash Health/Hudson Institute of Medical Research on tumor DNA extracted from either fresh frozen tissue or formalin-fixed, paraffin-embedded (FFPE) specimens provided as scrolls/shavings (10 μm thick) or fixed onto slides. The predominant specimen type was FFPE scrolls or shavings. Specimens containing at least 50% tumor content or higher were requested, with tumor content estimated by anatomic pathologists at the local site. On occasion, tumors with lower content were tested if optimal specimen was not available. All patients received standard-of-care histopathologic diagnosis. Immunohistochemistry and focused molecular testing followed local institutional guidelines and varied from site to site.

DNA from fixed tissue sections was extracted using the Reliaprep FFPE gDNA Miniprep System (Promega, Madison, WI), and DNA from fresh frozen tissue was extracted with the Blood and Tissue DNA extraction kit (Qiagen, Hilden, Germany), according to the manufacturer's instructions. Published studies had previously demonstrated there are no significant differences in classification outcomes following formalin fixation,¹¹ and these findings were confirmed in the authors' hands in a small tumor series. The median DNA concentration obtained was 87 ng/ μL , with a 95th percentile range from 4.63 to 392.00 ng/ μL . DNA concentrations were measured using fluorimetry on a Quantus Fluorimeter with Promega QuantiFluor ONE dsDNA dye. Typically, 500 ng was used for bisulfite conversion; however, on occasion, where insufficient material was available, a minimum of 198 ng was used. DNA extracted from specimens was evaluated for quality using a real-time quantitative PCR assay from Illumina (Infinium HD FFPE QC Assay Kit), according to the manufacturer's instruction.

Samples from all 11 Australian and New Zealand Children's Hematology/Oncology Group sites were in the following distribution: Royal Children's Hospital (Melbourne, Australia), 84 cases (29.5%); Monash Children's Hospital (Melbourne, Australia), 34 cases (12.3%); Perth Children's Hospital (Nedlands, Australia), 31 cases (10.8%); Queensland Children's Hospital (Brisbane, Australia), 31 cases (10.4%); Sydney Children's Hospital (Randwick, Australia), 24 cases (9.0%); Women's and Children's Hospital (Adelaide, Australia), 21 cases (7.8%); Starship Children's Hospital (Auckland, New Zealand), 17 cases (6.0%); The Children's Hospital at Westmead (Sydney, Australia), 16 cases (6.0%); John Hunter Children's Hospital (New Lambton Heights, Australia), 10 cases (3.7%); Royal Hobart Hospital (Hobart, Australia), 7 cases (2.6%); and Christchurch Hospital (Christchurch, New Zealand), 5 cases (1.9%).

Tumor histology, immunohistochemistry, and molecular analyses were performed and evaluated by local participating sites before specimen submission. Tumors fell within

the nine broad histologic categories described in the 2016 WHO classification.¹ Specimens for downstream processing comprised 230 FFPE blocks or shavings/scrolls, 37 FFPE sections on slides, 11 fresh frozen tumor samples, and 2 samples of DNA extracted at the treating site (1 from fresh frozen and 1 from FFPE tissue). DNA suitable for processing to DNA methylation analysis was successfully obtained from 269 of 280 (96%) samples. An informed judgment was made for progression of low DNA concentration specimens (<10 ng/ μL) based on sample availability. *O*⁶-methylguanine-DNA methyltransferase (*MGMT*) methylation-sensitive PCR (MS-PCR) quality checks for successful bisulfite conversion were affirmative in 265 of 269 (98.5%) cases, and 4 samples (1.5%) gave borderline *MGMT* MS-PCR quality control results. Where possible, DNA extraction and/or bisulfite conversion was successfully repeated in these cases, and they were progressed to array hybridization with satisfactory results.

Bisulfite Conversion

Approximately 500 ng DNA was subjected to bisulfite conversion using commercial kits, including the Methyl-Easy Xceed Kit (ME002; Human Genetic Signatures, Sydney, NSW, Australia) and the Zymo EZ DNA methylation kit (Zymo Research, Irvine, CA), according to the manufacturer's instruction, including Zymo's recommended cycling modifications for Illumina Infinium assays. All bisulfite-converted DNA samples and controls were subjected to an MS-PCR assay using a portion of the *MGMT* gene promoter sequence as a marker for bisulfite conversion.^{12,13} Primers for the amplification of unmethylated DNA and methylated DNA were from Christians et al¹³: water, 100% CpG methylated DNA (D5011; Zymo Research), and normal brain unmethylated DNA (D5018-1; Zymo Research) were used as controls and were bisulfite converted in parallel with samples for analysis. Cycling was at: 95 °C for 15 minutes, followed by 35 cycles of 95 °C for 30 seconds/59 °C for 30 seconds/72 °C for 30 seconds, and 1 cycle of 72 °C for 10 minutes. Specimens with successful bisulfite conversion amplified a 93-bp unmethylated band and/or an 81-bp methylated band when visualized on 2% agarose gels. The MS-PCR assay in the MethylEasy Xceed Kit was also used to identify bisulfite conversion in a large series of samples ($n = 92$) in parallel with the *MGMT* MS-PCR assay, before the exclusive use of the *MGMT* MS-PCR assay. As no differences in assay outcomes were identified, a decision was made to test bisulfite conversion using only the *MGMT* promoter assay for all subsequent specimens.

Restoration and Array Hybridization

Samples with qualitative evidence for adequate bisulfite conversion at a minimum concentration of 12.5 ng/ μL (100 ng in 8 μL) were then restored before array hybridization using the Illumina Infinium HD FFPE DNA Restore Kit

following the manufacturer's instructions. This step is not required for tumor DNA specimens isolated from unfixed frozen tissue; and for these samples, a minimum of 100 ng of DNA was submitted for array hybridization. Restored specimens were then sent to the Australian Genome Research Facility's Genomics Laboratory for array hybridization on the 850 K Infinium HD EPIC Methylation Array Bead Chip. The Australian Genome Research Facility is a National Association of Testing Authorities-accredited research facility and an Illumina Certified Service Provider for the Infinium Genotyping service. The Illumina Certified Service Provider program is a collaborative service partnership ensuring Illumina's best practices are adhered to. Data analysis was performed using Illumina's GenomeStudio version 2011.1 with methylation module 1.9.0 software, using the default Illumina settings and current Illumina manifest file for the Array Beach Chip.

Methylation Classifier

Data in the form of a zipped.idat file were made available for download from the Australian Genome Research Facility website. Unzipped.idat files for each specimen were then uploaded to the DKFZ brain tumor classifier version 11b4 (<https://www.molecularneuropathology.org>). Reports for tumor classifications were typically available within 24 hours. This interface accesses previously published classification algorithms and reference data sets.^{5,11} Consistent with previous studies, tumors were considered to classify reliably if their classification score was ≥ 0.90 . Closest classifications were also reported where scores of < 0.90 were obtained, with a caveat as to their reliability. Tumors classifying as medulloblastoma ≥ 0.90 were also evaluated on the medulloblastoma group 3 and 4 classifier¹⁴ version 1.0 for further subtyping into subgroups, I to VIII. A later version of the classifier, version 12.5, now incorporates these medulloblastoma subgroups and was used for retrospective analyses. The expanded classifier version 12.5 also includes germinomas, which were not represented on version 11b4. Hence, total tumor numbers classified on version 12.5 have a denominator value increased by four compared with those classified using version 11b4.

Reporting

Using classifications generated by the DKFZ classifier version 11b4, interpreted reports were prepared for each enrolled case. These reports included the primary DKFZ classification report, which included a chromosomal copy number profile. Reports were checked and validated by a senior investigator before upload to the REDCap patient database, from where they were distributed to the treating physician.

Next-Generation Sequencing

Next-generation sequencing using a custom panel was either conducted as part of the Molecular Neuropathology 2.0 (MNP2.0) study¹⁵ or completed as part of AB. Where sequencing occurred as part of AB, a 228-gene panel incorporating loci described in the MNP2.0 study plus additional genes was tested. The list of genes is described in [Supplemental Table S1](#). Libraries were prepared from 75 ng input DNA using SOPHiA Genetics library preparation reagents and custom probes, according to the manufacturer's instructions. Libraries underwent 151-bp paired-end sequencing on an Illumina NextSeq 550 at the Monash Health Translation Precinct Medical Genomics Core Facility. The SOPHiA Genetics DDM Platform was used for analysis of sequence data, curation of variants, and results reporting. A total of $97.52\% \pm 4.90\%$ of covered regions was sequenced to a depth of $1000\times$, with mean on-target rates of $78.31\% \pm 1.24\%$. A minimum variant allele frequency of 8% and read depth of 100 were required for variants to proceed to curation and reporting. Gene fusions could not be detected using this analysis platform. Mutations are described in Human Genome Variation Society format (<https://varnomen.hgvs.org>, last accessed May 30, 2023) with relevant reference sequences, including their release date in the National Center for Biotechnology Information (NCBI) GenBank. Reference sequences were last accessed on May 26, 2023.

Validation Series

Interlaboratory test validation was performed via the comparison of results from 104 participants co-enrolled on AB and MNP2.0 between March 2018 and July 2020. MNP2.0 analyzed FFPE blocks and tissue sections and included central neuropathology review, DNA methylation array, and additional molecular analyses, if required. The Australian and New Zealand Children's Hematology/Oncology Group acted as the MNP2.0 study sponsor in Australia and New Zealand and received all MNP2.0 results for comparison and distribution. MNP2.0 and AB reports were collated for each participant, and the methylation-based tumor classification and scores were compared.

The results from samples tested by MNP2.0 were not known until AB test results were reported because of the need to blind the testing and time differences in the turnaround time for generating results. AB results were typically reported to clinical trial investigators before those obtained from MNP2.0 (AB mean, 40 days; MNP2.0 mean, 68 days).

Statistical Analysis

Calculations of χ^2 and significance values were calculated for tumor score distributions using online analysis tools (<https://socscistatistics.com>, last accessed August 8, 2022). Associations were calculated using a 2×2 contingency

table with Yates correction. Where relevant, sample numbers were reported as the arithmetic mean with SD. Data were visualized using R.¹⁶

Results

Patient Enrollment

A total of 280 patients were enrolled in the AB study from October 2017 to June 30, 2021 (161 male and 119 female patients). The mean age was 8.53 years (SD, 5.45 years), which ranged from 15 days to 20.75 years. From these patients, tumor DNA sufficient for methylation profiling was obtained from 269 (96%) cases.

Concordance with Local Histopathology

Samples with DNA suitable for DNA methylation profiling were classified histologically, according to 2016 WHO CNS classification criteria. Ancillary molecular testing and immunohistochemistry were completed for many samples; however, the nature and extent of this varied across the 11 submitting sites. The distribution of histology classifications is shown in Table 1. Seven tumors could not be definitively diagnosed, including one tumor described as a high-grade pleomorphic lesion without distinguishing diagnostic features (A8382), one tumor in a patient with NF1 (A7519), a tumor with no definitive diagnosis (A8759), a tumor described as diffuse midline glioma with H3K27ME3 loss and MYCN amplification, not elsewhere classified (A1829), another possible tumor where the lesion was described as florid spongiosis leukoencephalopathy (C2539), one tumor with a differential diagnosis of myxoid glioneuronal tumor or pilocytic astrocytoma (A5103), and a low-grade glioma, nondiffuse tumor with H3K27 mutation and loss of trimethylation (A2425), for which a definitive diagnosis was challenging. Four germ cell tumors were excluded from inclusion in the data derived using classifier version 11b4 as this diagnosis was not represented on this methylation classifier version, leaving a total of 265 tumors that were potentially classifiable. Germinoma numbers were included when tumors were analyzed on classifier version 12.5, giving a total of 269 (see under classifications on DKFZ classifier 12.5).

Of 265 tumors classified by methylation using classifier version 11b4, 176 (67%) were classified with a score of ≥ 0.90 . Of these tumors, 162 of 176 (92%) were in agreement with their histologic diagnosis (as defined by WHO 2016 group classifications). Two tumors classifying histologically as other scored ≥ 0.90 and could not be compared, and five samples had control tissue classifications ≥ 0.9 . Seven of 174 (4.0%) samples with scores ≥ 0.90 (excluding two tumors unclassifiable by histology), classified using version 11b4, had discordant histopathology and methylation profiling classifications (Table 2). Three additional tumors had revised classifications to new tumor types not

represented in WHO 2016 but represented on the methylation classifier and in WHO 2021 and were not considered to be truly discordant, although their classifications changed (Table 3). One additional tumor (A2425) was categorized as other with a descriptive histology of nondiffuse glioma with H3K27M mutation and was considered consistent with methylation classifying it as a diffuse midline glioma with H3K27M mutation, as there was a suggestion in the histology report of regions that were potentially diffuse. It was not considered discordant and is not included in Table 2. Two tumors in Table 2 were found to carry mutations supporting the revised diagnosis, including platelet-derived growth factor receptor-A NM_006206.6: c.3144_3145del, p.(Ala1049Hisfs*2) (NCBI GenBank, <https://www.ncbi.nlm.nih.gov/genbank>, last accessed February 8, 2023), detected in tumor C6432, classifying as a glioblastoma IDH wild type, subtype RTKIII, and the fusion c11orf95(ZFTA)-RELA in C3139, classifying as an ependymoma, subtype RELA fusion. BRAF NM_004333.6: c.1799T>A, p.(Val600Glu) (NCBI GenBank, <https://www.ncbi.nlm.nih.gov/genbank>, last accessed April 10, 2023), was detected in C1432, a low-grade glioma/midline pilocytic astrocytoma that was originally diagnosed as a ganglioglioma; however, BRAF V600E is not exclusively associated with either diagnosis, although it does occur more frequently in ganglioglioma. The remaining reclassified tumors represented in Table 2 were not associated with specific diagnostic mutations.

Methylation profiling classified five tumors (A5928, C2539, A5463, A6028, and A6577) as control tissue, hemispheric cortex, or cerebellar hemisphere, indicative of low tumor content (<10%). This was confirmed in two specimens (A6577 and A5463). Including the control tissue classifications, 12 of 174 tumors (6.8%) had methylation classifications discordant with their histology, and a further 3 of 174 (1.7%) had revised and updated classifications but were not considered truly discordant.

Of the revised cases classified on 11b4 and shown in Tables 2 and 3, three cases proceeded to a study molecular tumor board consisting of the primary oncologist, site pathologist, and study team members (including J.R.H., N.G.G., E.M.A., C.L.W., and study pathologists) who reviewed the original histopathology (minimum two). For those who did not receive full molecular tumor board review, individual clinicians were consulted to confirm this decision. In one of the three reviewed cases, C2014, the methylation classification was accepted as representative of a new entity; in another case, C1432, the histology was accepted as being more reliable by the study pathologists because of the possibility of intratumoral heterogeneity in the region sampled for methylation testing, which may have impacted results; and in a third case, A9619, the sample was considered to align more closely on histopathology to a neurofibroma rather than a schwannoma. Analysis of the copy number variation plot did not identify changes in the NF1 locus to further adjudicate this case.

Table 1 Distribution of Histology of Tumors Progressing to Methylation Profiling

Histology group	Histology subgroup	Tumor grade	N	
Diffuse astrocytic and oligodendroglial (<i>n</i> = 38)	Anaplastic astrocytoma	III	6	
	Diffuse astrocytoma IDH mutant	II	1	
	Diffuse astrocytoma IDH wild type	II	1	
	Diffuse astrocytoma IDH wild type	III	1	
	Diffuse astrocytoma NOS	II	7	
	Diffuse astrocytoma NOS	III	1	
	Diffuse midline glioma	IV	2	
	Giant cell glioblastoma	IV	2	
	Glioblastoma IDH wild type	IV	3	
	Glioblastoma NOS	IV	12	
	Oligodendroglioma NOS	II	2	
	Other astrocytic tumors (<i>n</i> = 52)	Anaplastic pleomorphic astrocytoma	III	2
		Pilocytic astrocytoma	I	45
Pleomorphic xanthoastrocytoma		II	3	
Subependymal giant cell astrocytoma		I	2	
Neuronal and mixed neuronal glial tumors (<i>n</i> = 27)		Dysembryoplastic neuroepithelial tumors	I	8
	Ganglioglioma	I	11	
	Anaplastic ganglioglioma	III	2	
	Desmoplastic infantile astrocytoma and ganglioglioma	I	2	
	Papillary glioneuronal tumor	IV	1	
	Rosette-forming glioneuronal tumor	I	1	
	Diffuse leptomeningeal glioneuronal tumor	Not defined	2	
	Choroid plexus tumors (<i>n</i> = 6)	Choroid plexus papilloma	I	1
		Atypical choroid plexus papilloma	II	3
		Choroid plexus carcinoma	III	2
Embryonal tumors (<i>n</i> = 90)		Medulloblastoma WNT activated	IV	2
	Medulloblastoma SHH-activated <i>TP53</i> mutant	IV	1	
	Medulloblastoma SHH-activated <i>TP53</i> wild type	IV	4	
	Medulloblastoma non-WNT/non-SHH	IV	27	
	Medulloblastoma group 3	IV	1	
	Medulloblastoma, classic	IV	18	
	Medulloblastoma desmoplastic nodular	IV	4	
	Medulloblastoma nodular	IV	1	
	Medulloblastoma large-cell anaplastic	IV	5	
	Medulloblastoma NOS	IV	8	
	Embryonal tumors with multilayered rosettes C19 MC altered	IV	2	
	Embryonal tumors with multilayered rosettes NOS	IV	1	
	CNS ganglioneuroblastoma	IV	1	
	CNS embryonal tumor NOS	IV	3	
	Atypical teratoid rhabdoid tumor	IV	11	
	Embryonal tumor subtype not defined	IV	1	
	Tumors of the cranial and paraspinal nerves (<i>n</i> = 3)	Schwannoma	I	1
		Neurofibroma	I	1
		Perineurioma	I	1
	Meningiomas (<i>n</i> = 3)	Meningioma	I	1
Meningioma		II	1	
Atypical meningioma		I	1	
Mesenchymal nonmeningiothelial (<i>n</i> = 1)	Ewing sarcoma/PNET	NA	1	
Germ cell tumors (<i>n</i> = 4)	Mature teratoma	Not defined	1	
	Germinoma	II	2	
	Mixed germ cell tumor	Not defined	1	
Tumor of the sellar region (<i>n</i> = 1)	Adamantinomatous craniopharyngioma	I	1	

(table continues)

Table 1 (continued)

Histology group	Histology subgroup	Tumor grade	N
Tumors of the pineal region (n = 2)	Pineoblastoma	IV	2
Other gliomas (n = 4)	Angiocentric glioma	I	3
	Astroblastoma	Not applicable	1
Ependymomas (n = 31)	Myxopapillary ependymoma	I	1
	Ependymoma	II	14
	Ependymoma <i>RELA</i> positive	II	1
	Anaplastic ependymoma	III	15
Other (n = 7)			7
Total			269

Of 280 tumor samples received, 269 had sufficient quantity and quality of DNA to proceed to methylation profiling.
CNS, central nervous system; NOS, not otherwise specified.

Of the 162 samples showing concordance between histology group classification and methylation classification, seven were either discordant or lacked clarity at the subgroup level. In two of these cases, A5705 and A5269, diagnosed histologically as SHH medulloblastoma and medulloblastoma with classic histology, respectively, a more refined diagnosis by histology was problematic because of technical difficulties; however, they were both classified by methylation profiling as being WNT-activated medulloblastoma, and sequencing identified *CTNNB1* mutations in both tumors (*CTNNB1* NM_001904.4: c.100G>A, p.Gly34Arg; and *CTNNB1* NM_001904.4: c.94G>A, p.Asp32Asn; NCBI GenBank, <https://www.ncbi.nlm.nih.gov/genbank>, last accessed May 15 2023), supporting this classification. In a third tumor, A8721,

histology was done on a frozen section with a diagnosis of a poorly differentiated ependymal tumor with neuroepithelial features, which was shown by methylation profiling to match the more refined diagnosis of a *RELA* fusion subtype ependymoma. Two further tumors, C7239 and C9805, were originally classified as diffuse astrocytoma WHO grade II, with one subsequently shown by methylation classification to be a GBM IDH wild type, subclass RTKIII, and the other to be a glioma, IDH mutant sub-class 1p/19q codeleted oligodendroglioma. Another medulloblastoma, C3673, was diagnosed histologically as belonging to the SHH subclass A, yet methylation profiling showed that it belonged to SHH subclass B. Finally, tumor A6312 was diagnosed as a low-grade glioneuronal tumor with histologic features most in keeping

Table 2 Tumors with Methylation Classifications Discordant with Histology Obtained Using Classifier 11b4

Tumor no.	Local histopathologic diagnosis (according to 2016 WHO main and subgroup classification ¹)	Methylation classification on classifier version 11b4	Comment
A6432	Ependymal tumor/anaplastic ependymoma	Glioblastoma IDH wild type, subtype RTKIII	Discordant
C3139	Other astrocytic/pleomorphic xanthoastrocytoma grade III	Ependymoma, subtype <i>RELA</i> fusion	Discordant
A6896	Ependymal/ependymoma	Papillary tumor of the pineal region	Discordant
A9619	Other glioma/NF1 neurofibroma	Schwannoma	Discordant
A3406	Other astrocytic/pilocytic astrocytoma grade I	Low-grade glioma/dysembryoplastic neuroepithelial tumor	Discordant
C1432	Neuronal and mixed neuronal glial tumor/gangliocytoma, ganglioglioma grade I; piloid features noted in tumor	Low-grade glioma/midline pilocytic astrocytoma	Discordant
A8658	Embryonal NOS	CNS Ewing sarcoma family tumor with <i>CIC</i> alteration	Discordant; new classification on WHO 2021 ³ but belongs in the group mesenchymal, nonmeningothelial tumors

Re-evaluation of these classifications using classifier 12.5 gave results consistent with 11b4 classification for all tumors, except A3406, which classified within the type low-grade glial/glioneuronal/neuroepithelial as subtype low-grade glioneuronal tumor on 12.5 with a score ≥ 0.90 .

CNS, central nervous system; NOS, not otherwise specified; WHO, World Health Organization.

Table 3 Tumor Samples with Updated Classification

Tumor no.	Local histopathologic diagnosis (according to 2016 WHO main and subgroup classification ¹)	Methylation classification on classifier version 11b4	Comment
C9165	Diffuse astrocytic and oligodendroglial tumor/glioblastoma grade IV NOS	CNS neuroblastoma with <i>FOXR2</i> activation	New classification
A5494	Diffuse astrocytic and oligodendroglial tumor/anaplastic astrocytoma IDH wild type grade IV	CNS neuroblastoma with <i>FOXR2</i> activation	New classification
C2014	Neuronal and mixed neuronal glial/glioneuronal NOS/?pilocytic astrocytoma	CNS neuroblastoma with <i>FOXR2</i> activation	New classification

These were samples where the tumor type was not represented in WHO 2016, but subsequently represented in WHO 2021³ and on classifier 11b4. These samples were not considered to be truly discordant with histology.

CNS, central nervous system; NOS, not otherwise specified; WHO, World Health Organization.

with dysembryoplastic neuroepithelial tumor WHO grade I, but was found by methylation profiling to belong to the subgroup rosette-forming glioneuronal tumor. Inclusive of group and subgroup discrepancies and considering only tumors with classification scores ≥ 0.90 , the overall concordance between methylation profiling classification and histology was 155 of 176 (88%).

Medulloblastoma and low-grade glioma were the most frequent classifications, consistent with their incidence in the pediatric population. Meningioma, oligodendroglioma IDH mutant with 1p/19q codeletion, and Ewing sarcoma classifications were the least common. Figure 1 shows the distribution of classifications obtained.

Methylation Profiling Significantly Refines Tumor Subgroup Classifications

Methylation profiling yielded molecular information, refining tumor diagnosis in 130 of 176 (74%) of cases with scores of ≥ 0.90 on 11b4 when compared with histology. This information was grouped into three categories, including the following: i) the presence of a chromosomal change or fusion gene [$n = 21$ cases (16%)], ii) a subgroup associated with a specific mutation [$n = 51$ cases (39%)], and iii) a more detailed description of the tumor subclass [$n = 64$ cases (49%)]. Six (5%) tumors were assigned to more than one category. Examples of tumors with fusion genes included low-grade gliomas with *KIAA1549-BRAF* and ependymomas with *c11orf95-RELA* (*ZFTA-RELA*), where these were inferred from copy number variation plots. Tumor subclasses associated with the presence of specific mutations included the glioblastoma IDH wild-type subclass H3.3 G34R, WNT, and SHH subtypes of medulloblastoma and subgroups of atypical teratoid/rhabdoid tumor. Tumors where methylation classification provided more information included non-WNT/non-SHH medulloblastomas classed as either group 3 or group 4.

On classifier 11b4, methylation subclassifications for medulloblastoma identified five subgroups in 65 tumors

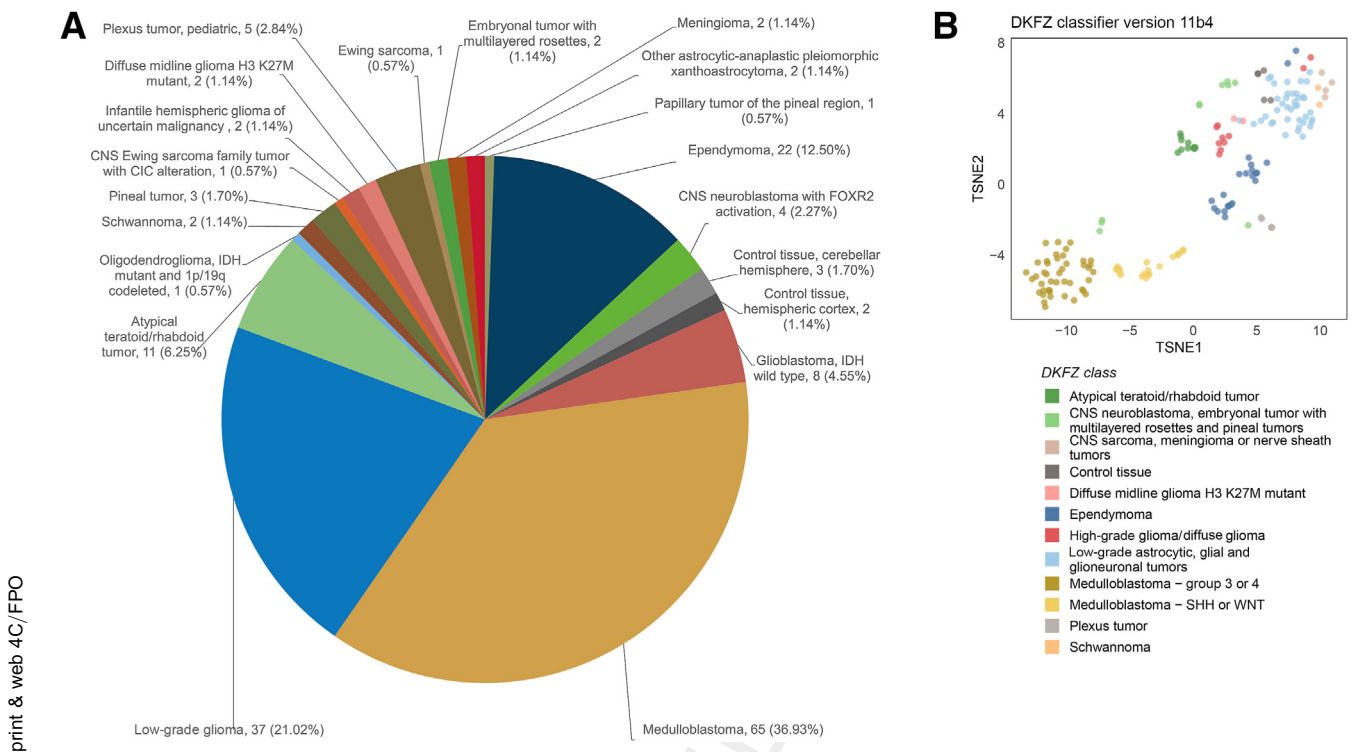
with classification scores of ≥ 0.90 . Group 4 was the most common ($n = 28$), and the WNT subgroup the least common ($n = 7$) (Figure 2A). Of the remaining cases, seven tumors belonged to the SHH A subgroup, and seven belonged to the SHH B subgroup. Medulloblastomas classifying ≥ 0.90 belonging to group 3 or group 4 were also evaluated on the DKFZ medulloblastoma classifier version 1.0. Of 33 tumors with subclassification scores ≥ 0.90 , seven subtypes were identified, as shown in Table 4, with subtypes II, VII, and VIII occurring the most frequently.

On classifier 11b4, low-grade gliomas ($n = 37$) classified into eight distinct subgroups, with the most frequent classifying as posterior fossa pilocytic astrocytoma and the least frequent classifying as rosette-forming glioneuronal tumor, ganglioglioma, and tumors with *MYB/MYBL1* rearrangement (Figure 2B). Ependymomas ($n = 22$) were classified into four subgroups, with posterior fossa group A and *RELA* (later referred to as *ZFTA*) fusion tumors representing the most frequent subgroups (Figure 2C). Three subgroups of atypical teratoid/rhabdoid tumor ($n = 11$) were represented on the classifier, and the most frequent was the SHH subgroup (Figure 2D).

Tumors Below the Classification Threshold

Of 265 tumors, 64 (24.1%; excluding $n = 2$ germinomas) classified with a score of between 0.30 and 0.89 on classifier 11b4. Low-grade gliomas were the most frequently occurring tumor type among these [$n = 25$ (40%)]. For 36 (56%) tumors not classifying > 0.90 , the closest match classification was consistent with the histologic diagnosis. Seven cases (11%) classified as control tissue below the 0.90 threshold. These included hemispheric cortex, reactive brain, hypothalamus, or inflammatory tissue classifications. This is indicative of low tumor content; however, in several instances, the tumor was described as diffuse or diagnostically challenging.

When the tumor content was compared across subgroups with scores in the range from 0.30 to 0.89, derived using



print & web 4C/FPO

Figure 1 Tumor classifications with scores ≥ 0.90 . Classification scores ≥ 0.90 were obtained for 176 tumors on classifier 11b4. **A:** Most of these samples classified as medulloblastomas, low-grade gliomas, or ependymomas. Low-grade gliomas included posterior fossa pilocytic astrocytomas, midline pilocytic astrocytomas, dysembryoplastic neuroepithelial tumors, subependymal giant cell astrocytomas, desmoplastic infantile astrocytomas, *MYB/MYBL1*-altered tumors, rosette-forming glioneuronal tumors, hemispheric pilocytic astrocytoma, and gangliomas. **B:** TSNE analysis showed clustering of related tumors. CNS, central nervous system; DKFZ, Deutsches Krebsforschungszentrum (German Cancer Research Center).

classifier 11b4, there were no significant differences in mean \pm SD tumor content in those classifying, with scores from 0.30 to 0.49 ($64\% \pm 23\%$), 0.50 to 0.74 ($67\% \pm 18\%$), and 0.75 to 0.89 ($59\% \pm 20\%$). Indeed, tumors with scores in the higher range had slightly lower tumor content. (For this calculation, tumors cited as having content $>50\%$ were assigned a value of 51%; hence, mean values for tumor content were conservative estimates.) However, tumors classifying ≥ 0.90 had a higher mean tumor content of $85\% \pm 15\%$, suggesting that some tumors with classifications below the threshold value of 0.90 may have lower scores because of reduced tumor content.

Tumors without a Classification by Methylation Profiling

Twenty-five of 265 (9.4%) tumors (excluding $n = 2$ germ cell tumors) were below all classification thresholds (cutoff value, 0.30) when evaluated on classifier 11b4. Low tumor content could not be excluded as a reason for non-classification in 11 cases because the tumor content of the specimen tested was either unknown or known to be $<50\%$. However, as a normal tissue classification was not indicated in any of these specimens, it is not possible to be definitive about the reason for non-classification. However, 14 cases had a tumor content of $>50\%$ and a mean content overall of

$72\% \pm 23\%$. [Supplemental Table S2](#) shows the WHO 2016 group and subgroup of tumors that did not classify with a score of >0.30 .

Test Quality Issues

Scattered Data

During the course of the study, scattering of methylation array data could lead to lower classification scores and failure to classify. When this occurred, the array CpG count was consistently lower than the median of approximately 835,000 CpG at a confidence of 0.01. This was noted in five samples [5/269 (1.8%)]. Retesting of these samples yielded scores of >0.90 in four cases. However, although two of these specimens did not match any tumor class on first-round testing, and had scores of <0.31 , they subsequently were classified as pilocytic astrocytoma, with scores of 0.98 and 0.99. A third tumor classified as a low-grade glioma *MYB/MYBL1* with a score of 0.33, and on repeated testing, yielded a score of 0.99 with the same classification; however, a fourth tumor had a closest match classification with a score of 0.57 to a choroid plexus tumor, and on repeated testing, classified as an atypical teratoid/rhabdoid tumor with a score of 0.98. This changed classification with better data emphasizes the importance of generating high-quality array data and relying only on tumor classifications with scores ≥ 0.90 . In the

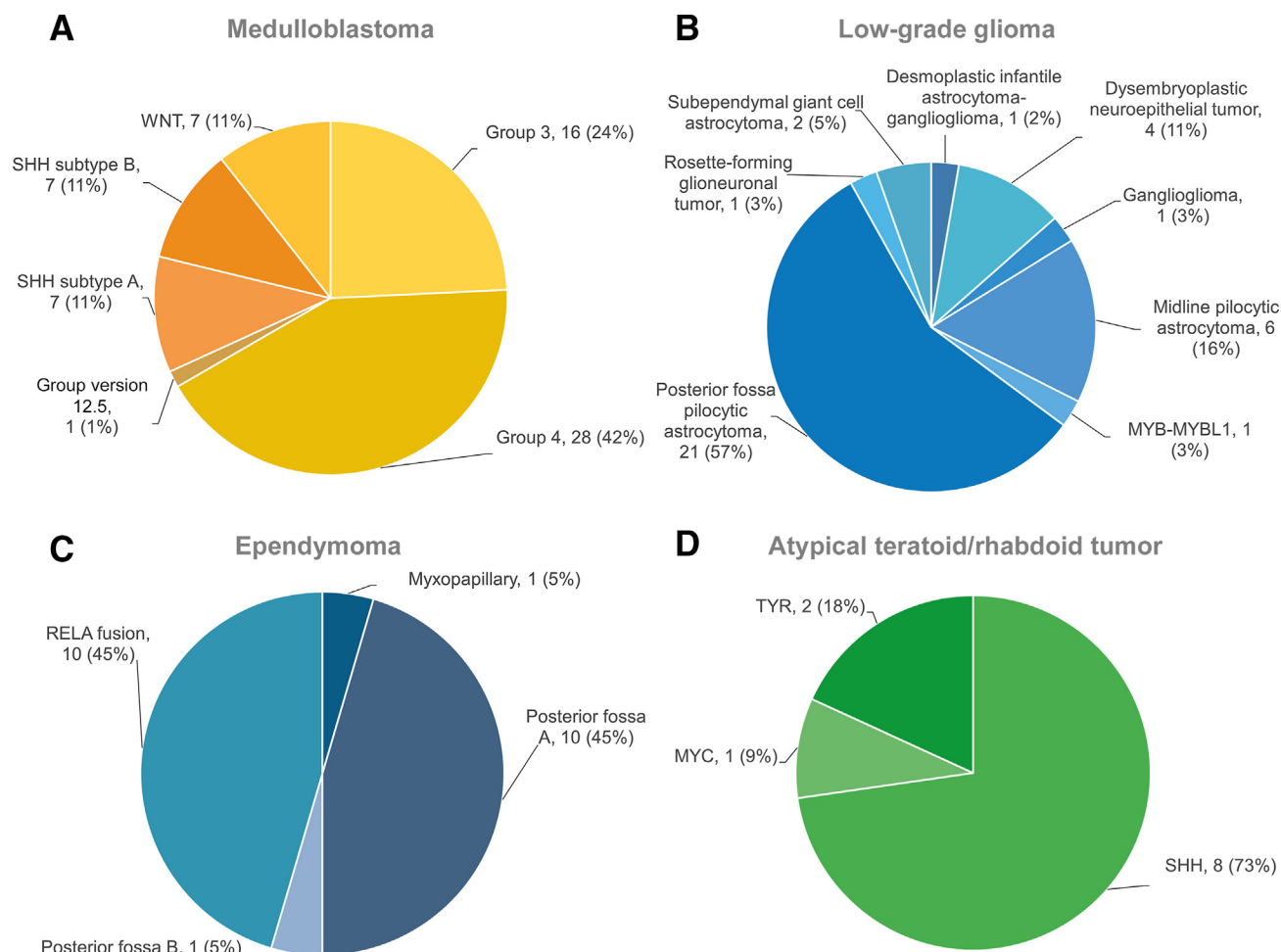


Figure 2 Tumor subclassifications with scores ≥ 0.90 on classifier version 11b4. Methylation array profiling allowed additional subclassification of tumors with scores ≥ 0.90 . **A:** A total of 66 medulloblastoma samples with scores ≥ 0.90 were further subclassified into group 4 [28 (42%)], group 3 [16 (24%)], SHH A [7 (11%)], SHH B [7 (11%)], and WNT [7 (11%)] medulloblastomas on classifier 11b4. One additional group 4 tumor was classified on 12.5 and not on 11b4 2.0 and is shown separately. **B:** A total of 37 low-grade glioma samples scored ≥ 0.90 on classifier 11b4 2.0 and were further subclassified into posterior fossa pilocytic astrocytomas [21 (57%)], midline pilocytic astrocytomas [6 (16%)], dysembryoplastic neuroepithelial tumors [4 (11%)], subependymal giant cell astrocytomas [2 (5%)], and desmoplastic infantile astrocytoma, *MYB/MYBL1*, rosette-forming glioneuronal tumor, and ganglioma [each 1 (3%)]. **C:** A total of 22 ependymoma samples with scores ≥ 0.90 on classifier 11b4 were further sub-classified into *RELA* fusion [10 (45%)], myxopapillary [1 (5%)], posterior fossa group A [10 (45%)], and posterior fossa group B [1 (5%)] ependymomas. **D:** A total of 11 atypical teratoid/rhabdoid tumor samples with scores ≥ 0.90 on 11b4 were further sub-classified into SHH [8 (73%)], TYR [2 (18%)], and MYC [1 (9%)] sub-groups.

remaining case, array data were not improved by repeated testing and scores >0.90 were not obtained.

Bias

If it is assumed that the classifier has capacity to classify all tumors equivalently, then WHO tumor groups would be expected to have a similar proportional representation in the classifiable versus non-classifiable categories, assuming equivalence in sample quality and tumor content across different tumor groups. Table 5 shows the percentage of tumors in each major grouping that were classified with scores of >0.90 on the classifier version 11b4. As can be seen, most medulloblastomas, ependymomas, and atypical teratoid/rhabdoid tumors reveal the most robust classifications, in contrast to low-grade gliomas and glioblastomas, which are not as readily classifiable.

Quality Assurance

Comparison of Tumor Genomics

A total of 33 (19%) tumors with scores on methylation profiling >0.90 evaluated on classifier version 11b4 had prior testing by conventional cytogenetics, fluorescence *in situ* hybridization, or single-nucleotide polymorphism microarrays. When the results of these were compared to the copy number profiles generated by methylation profiles, 31 (94%) were either fully [22/33 (66.7%)] or partially consistent [9/33 (27%)] for gross chromosomal abnormalities. Partial consistency reflects technological limitations attributable to clonal abnormalities that are below detection threshold, copy number neutral alterations, focal amplifications, and translocations in the relevant cases. In two cases (6%), inconsistencies were noted between the

Table 4 Group 3 and Group 4 Medulloblastoma Subclassifications

Subtype	I	II	III	IV	V	VI	VII	VIII
Group 3	0	6	4	1	0	0	1	0
Group 4	0	0	0	0	4	1	7*	9

Tumors classifying as group 3 or group 4 medulloblastomas were further analyzed using the medulloblastoma group 3/4 subclassifier.

*Subtype VII included an additional tumor evaluated on classifier 12.5.

methylome copy number variation plot and diagnostic molecular cytogenetic reports.

Tumors classifying with evidence for the presence of a fusion gene had in some cases been ascertained by cytogenetic or molecular testing. Methylation classifications of pilocytic astrocytoma indicated the presence of *KIAA1549-BRAF* fusions from copy number variation plots in 16 tumors from a total of 27 with scores ≥ 0.90 . In 12 of these cases, the fusion had also been identified by other methods; however, not all cases had additional testing. Five tumors classifying as ependymoma subtype *RELA* fusion on methylation arrays had the fusion confirmed as *C11orf95-RELA* by sequencing.¹⁵ Results were in 100% agreement with the methylation classifications where this testing was done.

Sequencing of tumor DNA verified the subclass designations in all tumors sequenced where the presence or absence of a mutation was indicative of a subclass. A total of 159 tumors with scores ≥ 0.90 were sequenced. These included IDH1 mutant oligodendroglioma, glioblastoma IDH wild-type subclass H3.3 G34R, medulloblastoma WNT subclass, and medulloblastoma SHH subclasses, in which relevant pathogenic mutations were identified in *IDH1*, *H3F3A*, *TP53*, *CTNBN1*, *PTCH1*, and *SUFU* (Supplemental Table S3).^{14,17}

Comparative Testing

A total of 104 tumors underwent prospective concurrent testing in both the MNP2.0 DKFZ and AB trials, and 103 tumors had concordant classifications (99%), including classifications ≥ 0.90 , closest match classifications < 0.90 ,

Table 5 Distribution of Tumor Scores According to Their Closest Classification

Classification group	Score ≥ 0.90 , Score ≤ 0.90 ,		P value
	n (%)	n (%)	
Medulloblastoma	65 (93)	6 (7)	< 0.00001
Low-grade glioma	37 (60)	25 (40)	0.362
Ependymoma	22 (79)	6 (21)	0.051
Atypical teratoid/rhabdoid tumor	11 (85)	2 (15)	0.202
Glioblastoma IDH wild type	8 (61)	5 (38)	1.000

Significance P values (< 0.05) were calculated using a χ^2 analysis with Yates correction, assuming tumors in each group had an equivalent chance of classifying above or below 0.90.

and non-classifications. In one discordant case, C2592, different paraffin blocks from the same tumor were used as source material in each laboratory as insufficient material was available for direct cross-comparison from the same block. In AB, this tumor did not classify, but on MNP2.0, it classified as a low-grade glioma/posterior fossa pilocytic astrocytoma. In another case (C3077), which was not counted, tumors from different surgeries (relapse versus diagnosis) were tested in each laboratory. Table 6 shows the classification concordance obtained for tumor samples passing internal quality criteria and demonstrates excellent concordance between laboratories.

Classifier scores were examined across both studies for the 103 tumors with concordant methylation classifications. Scores ranged from 0.99 to a did not classify, generating a score ≤ 0.30 . For all scores, differences of < 0.10 occurred in 80 of 95 cases (84%). Score distributions are shown in Figure 3. Six samples tested on MNP2.0 gave scores ≥ 0.90 , whereas when tested on AB, the scores were < 0.90 for the same samples (Supplemental Table S4). Two samples scored 0.81 and 0.89 and were close to the 0.90 threshold value.

In summary, when the authors' data are compared with those of the DKFZ reference laboratory and a score cutoff of 0.90 is applied to the data, the authors achieve a 93% sensitivity (75/81) for achieving concordance in score thresholds.

Intralaboratory Variability

Intralaboratory variability for specimen DNA prehybridization processing and hybridization was assessed for six tumors with different histology, including atypical teratoid/rhabdoid tumor, medulloblastoma, glioblastoma, ependymoma, and choroid plexus tumor, where the processing steps for each tumor were undertaken and reproduced by a minimum of two technicians. Classifications and subclassifications ≥ 0.90 were highly concordant between operators. For choroid plexus tumors, minor variations were observed, with the assignment of subclassification to either pediatric A or pediatric B, both of which were close to the cutoff value of 0.50 for tumor subclassification.

Tumor Reclassifications on DKFZ Classifier 12.5

Following the recent release of classifier version 12.5 by DKFZ, all tumors ($n = 269$), including four germinomas, were re-evaluated. A total of 213 of 269 specimens scored ≥ 0.90 (79.2%). Of these specimens, 18 of 213 (8.4%) had classifications inconsistent with their histopathology, where a definitive descriptive diagnosis was made. These included three control tissue classifications, seven classifications that were not consistent with histopathology, as previously described in Table 2, and eight classifications from 12.5 analysis that were not consistent with histopathology, Table 7, at either group or subgroup level. One tumor in Table 2, A3406, had differing classifications on 11b4 and

Table 6 Concordance for Tumor Classifications between AIM BRAIN and MNP2.0 Studies

Tumors with any score ≥ 0.31 and a classification in both studies	Classification concordance (specificity), %	Tumors with score ≥ 0.90 in both studies	Classification concordance (specificity), %
95	99	75	100

Classifications derived from Deutsches Krebsforschungszentrum (German Cancer Research Center) classifier version 11b4 for tumors in both AIM BRAIN and MNP2.0 studies, where a classification was recorded, were compared.

MNP2.0, Molecular Neuropathology 2.0.

12.5, classifying ≥ 0.90 on 12.5 to the subtype low-grade glioneuronal tumor, and remained nonconcordant with histopathology. A further nine tumors had revised or new classifications on 12.5 that were not previously represented in WHO 2016 and were not considered strictly discordant. These included three (Table 3), four (Table 8), and two (Table 9) tumors.¹⁸

Of the discordant tumors represented in Table 7, one had some evidence for the revised classification status based on mutation screening. A1639, classifying as a diffuse pediatric-type high-grade glioma, H3 wild type, and IDH wild type, subtype A, had H3.3 and IDH1 wild-type status confirmed.

Samples with scores ≥ 0.90 on classifier version 11b4, when re-evaluated on classifier 12.5, did not give concordant class classifications in all cases, with 167 of 176 (95%) cases yielding concordant results for class and subclass. Interestingly, none of the five control tissue classifications identified on 11b4 scored ≥ 0.90 on 12.5. Tumors classifying < 0.90 on 12.5 but ≥ 0.90 on 11b4 included two diffuse high-grade gliomas, classified as glioblastoma IDH wild type on 11b4, and two choroid plexus tumors. When tumors with scores in the range 0.31 to 0.89 on classifier 11b4 ($n = 66$, including two germinomas) were re-evaluated using classifier version 12.5, 33 tumors of 66 samples reclassified with scores ≥ 0.90 . Three tumors within this group classified ≥ 0.90 as control tissue reactive tumor microenvironment, leaving 30 tumors classifying. Of the

tumors that did not classify using classifier version 11b4 and that scored ≤ 0.30 ($n = 27$, including two germinomas), 13 (including two germinomas) were reclassified ≥ 0.90 using classifier version 12.5. Of these 13 tumors, two (A9145 and C4495) had histology that was discordant with their methylation classification and are included in Table 7. Supplemental Table S5 outlines tumor numbers obtained for classification score groupings for both 11b4 and 12.5.

Nearly all tumors scoring < 0.90 on 11b4 that reclassified ≥ 0.90 on 12.5 were described in more detail, including 8 (19%) with a chromosomal change or fusion gene and 7 (17%) with a specific mutation. Classifications derived from 12.5 for the cohort are shown in Figure 4. On classifier 12.5, some tumor group and subgroup descriptions changed (Figure 4A). Subependymal giant cell astrocytoma, previously assigned as a low-grade glioma on 11b4, fell within the new group, circumscribed astrocytic tumors. Low-grade glial/glioneuronal/neuroepithelial tumors, ependymomas, and diffuse high-grade gliomas were also classified into multiple subgroups and subclasses on 12.5 that were more refined than those on 11b4 (Figure 5). Tumors either classifying > 0.90 or with a closet match classification as glioblastoma IDH wild type on 11b4 were reassigned on 12.5 as pediatric-type diffuse high-grade gliomas and subclassified into multiple subtypes (Figure 5C). The classification biases evident between tumor groups on 11b4 appear to have been reduced on 12.5, with a higher number of low- and high-grade gliomas

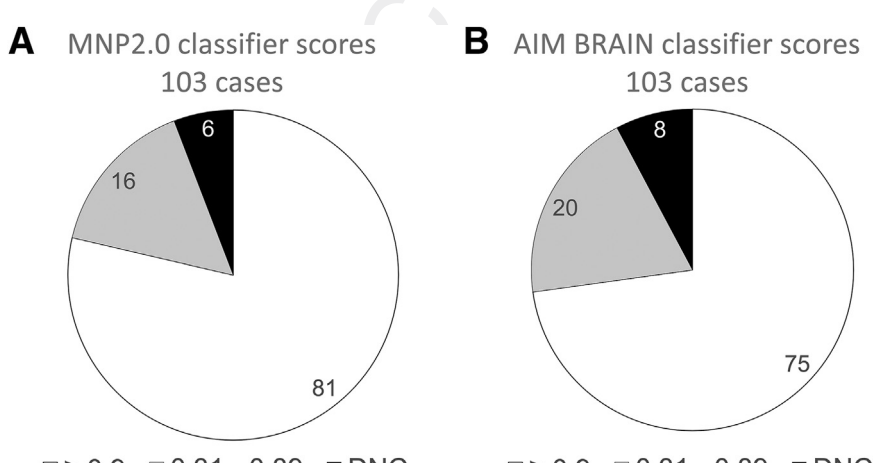


Figure 3 Score distribution and comparison of Molecular Neuropathology 2.0 (MNP2.0) and AIM BRAIN classifier results. A total of 103 samples were tested in parallel at Deutsches Krebsforschungszentrum (German Cancer Research Center) through MNP2.0 and in the local laboratory as part of AIM BRAIN. **A:** MNP2.0 testing classified 81 samples with scores ≥ 0.90 , 16 samples with scores in the range 0.31 to 0.89, and 6 samples with scores ≤ 0.30 . **B:** Parallel analysis through AIM BRAIN testing classified 75 samples with scores ≥ 0.90 , 20 samples with scores in the range 0.31 to 0.89, and 8 samples with scores ≤ 0.3 . DNC, did not classify.

Table 7 Reclassification of Discordant Tumors Using 12.5

Tumor no.	Local histopathologic diagnosis (according to 2016 WHO main and subgroup classification ¹)	Methylation classification on classifier version 12.5	Related group and subgroup WHO 2021 ³	Comment
A5654	Diffuse astrocytic and oligodendroglial tumor/anaplastic astrocytoma NOS, WHO grade III	Subtype pleomorphic xanthoastrocytoma of the type diffuse glioma MAPK altered cell cycle activated; high-grade astrocytoma with piloid features is a related subtype	Subtype pleomorphic xanthoastrocytoma of the type circumscribed astrocytic gliomas; high-grade astrocytoma with piloid features is a related subtype	Subtype discordance
C2310	Embryonal tumor/CNS embryonal tumor NOS, WHO grade IV	Supratentorial ependymoma, ZFTA fusion positive, subclass E; fusion confirmed by RNA-seq	Supratentorial ependymoma, ZFTA fusion positive	Type and subtype discordance
A7536	Neuronal and mixed neuronal glial tumor/ganglioglioma, WHO grade I	Subtype pilocytic astrocytoma hemispheric, of low-grade glial/glioneuronal/neuroepithelial tumors; ganglioglioma is also a subtype of low-grade glial/glioneuronal/neuroepithelial tumors	Subtype pilocytic astrocytoma of the type circumscribed astrocytic gliomas, whereas ganglioglioma is a subtype of glioneuronal and neuronal tumors	Differences between 12.5 and WHO 2021 type; subtype discordance
A7405	Neuronal and mixed neuronal glial tumor/dysembryoplastic neuroepithelial tumor, WHO grade I	Subtype pilocytic astrocytoma, hemispheric, of the type low-grade glial/glioneuronal/neuroepithelial tumors; dysembryoplastic neuroepithelial tumor is also a subtype of low-grade glial/glioneuronal/neuroepithelial tumors	Subtype pilocytic astrocytoma is of the type circumscribed astrocytic gliomas; dysembryoplastic neuroepithelial tumor falls within the separate type glioneuronal and neuronal tumors	Differences between 12.5 and WHO 2021 type and subtype classifications; subtype discordance
A1580	Diffuse astrocytic and oligodendroglial tumor/diffuse astrocytoma IDH wild type, WHO grade II	Subtype pilocytic astrocytoma infratentorial is of the type low-grade glial/glioneuronal/neuroepithelial tumors; on 12.5, some subtypes of diffuse astrocytoma fall within this type	Subtype pilocytic astrocytoma is of the type circumscribed astrocytic gliomas; diffuse astrocytoma IDH wild-type WHO grade II is no longer considered a type in WHO 2021	Subtype discordance
A9206	Neuronal and mixed neuronal glial tumor/ganglioglioma with areas of high-grade transformation, WHO grade III	Subtype pleomorphic xanthoastrocytoma is of the type diffuse glioma MAPK altered, cell cycle activated; gangliogliomas is of the type low-grade ganglioglioma and neuroepithelial tumors	Subtype pleomorphic xanthoastrocytoma is of the type circumscribed astrocytic tumors; gangliogliomas are a subtype of glioneuronal and neuronal tumors	Type and subtype discordance

(table continues)

Table 7 (continued)

Tumor no.	Local histopathologic diagnosis (according to 2016 WHO main and subgroup classification ¹)	Methylation classification on classifier version 12.5	Related group and subgroup WHO 2021 ³	Comment
A9145	Meningioma/atypical meningioma grade II	Ependymal tumor/subtype supratentorial <i>ZFTA-RELA</i> fusion-positive ependymoma, subclass E	Ependymal tumors/supratentorial ependymoma, <i>ZFTA</i> fusion positive	Type and subtype discordance
C4495	Ependymal tumor/anaplastic ependymoma grade III	CNS tumor with <i>BCOR/BCORL1</i> fusion	New subtype CNS tumor with <i>BCOR</i> internal tandem duplications in WHO 2021 under other CNS embryonal tumors	Type and subtype discordance

Tumors with methylation classifications discordant with histology, reclassified using classifier version 12.5, with scores ≥ 0.90 ($n = 8$). Of these tumors, six previously scored in the range 0.31 to 0.89 on 11b4, and two (A9145 and C4495) scored < 0.30 .

CNS, central nervous system; MAPK, mitogen-activated protein kinase; NOS, not otherwise specified; RNA-seq, RNA sequencing; WHO, World Health Organization.

now classifying. Only a single medulloblastoma rescored ≥ 0.90 on 12.5 (Figure 2A), with the vast majority already classifying ≥ 0.90 on 11b4. Overall, on 12.5, 42 of 269 tumors (15.6%) were below the classification threshold of 0.90, and 14 (5.2%) did not classify with a score of > 0.30 , giving an overall non-classification rate of 21% compared with 34% on 11b4.

A total of 14 tumors scored ≤ 0.30 when re-evaluated on 12.5. WHO 2016 groups and subgroups for tumors remaining with no closest match classification and scores ≤ 0.30 on both classifiers 11b4 and 12.5 are shown in Supplemental Table S2.

Thirteen tumors moved from a non-classification with scores ≤ 0.30 on 11b4 to a high confidence classification on

Table 8 New Tumor Types Confirmed Using 12.5 Classifier

Tumor no.	Local histopathologic diagnosis (WHO 2016 ¹)	Methylation classification 12.5	Related type and subtype (WHO 2021 ³)	Comment
A1639	Other gliomas/angiocentric glioma with focal anaplasia	Diffuse pediatric-type high-grade glioma, H3 wild type and IDH wild type, subtype A	New subtype on WHO 2021, diffuse pediatric-type high-grade glioma, H3 wild type and IDH wild type	New classification; <i>IDH1</i> and H3 wild type confirmed
C1030	Diffuse astrocytic and oligodendroglial/glioblastoma, WHO grade IV	Diffuse pediatric-type high-grade glioma, RTK1 subtype, subclass B	Pediatric-type diffuse high-grade gliomas	New classification; <i>PDGFRA</i> and <i>ARID1B</i> mutations detected
C4545	Embryonal/NOS	CNS embryonal tumor with <i>BRD4-LEUTX</i> fusion	Specific subtype not listed in WHO 2021; closest to other CNS embryonal tumors	New classification on 12.5
A4980	Diffuse astrocytic and oligodendroglial/glioblastoma, IDH wild type	Diffuse pediatric-type high-grade glioma, RTK1 subtype, subclass A	Pediatric-type diffuse high-grade gliomas	New classification on 12.5
C5390	Features of multiple low-grade glioma types, including pilocytic astrocytoma and subependymal giant cell astrocytoma	Subtype pilocytic astrocytoma, hemispheric of the type low-grade glial/glioneuronal/neuroepithelial tumors	Subtype pilocytic astrocytoma is of the type circumscribed astrocytic gliomas	Confirmed classification

Classifications where the tumor histology aligned with a new related category in WHO 2021 or in the 12.5 classification system and were not considered to be discordant with histopathology ($n = 4$). One additional tumor, C5390, did not belong to a new subtype, but 12.5 classification clarified the diagnosis.

CNS, central nervous system; NOS, not otherwise specified; WHO, World Health Organization.

Table 9 Tumor Reclassifications Using Version 12.5

Tumor no.	Local histopathologic diagnosis (according to 2016 WHO main and subgroup classification ¹)	Methylation classification on classifier version 12.5	Related WHO 2021 group and subgroup ³	Comment
C2073	Diffuse astrocytic and oligodendroglial tumor/giant cell glioblastoma grade IV	Neuroepithelial tumor with MN1-PATZ1 fusion	Consistent with new subtype based on molecular features astroblastoma MN1 altered in WHO 2021 under circumscribed astrocytic tumors	New classification; fusion confirmed by RNA-seq
A4751	Diffuse astrocytic and oligodendroglial tumor/glioblastoma NOS grade IV	Anaplastic neuroepithelioma with condensed nuclei	Tumor type is not represented in WHO 2021 but is present in update by Komori (2023) ¹⁸	New classification
C6235	Embryonal tumor/embryonal tumor with multilayered rosettes grade IV	Embryonal tumor with multilayered rosettes, non-C19 MC altered	No change in WHO 2021 classification	Concordant with histology
A9937	Neuronal and mixed neuronal glial tumor/papillary glioneuronal tumor grade IV	Subtype glioneuronal tumor subtype A of the group diffuse glioneuronal tumors	Subtype papillary glioneuronal tumor of the type glioneuronal and neuronal tumors	Concordant with histology
A8220	Other astrocytic tumor/pilocytic astrocytoma grade I	Pilocytic astrocytoma, midline	Subtype pilocytic astrocytoma of the type circumscribed astrocytic gliomas	Concordant with histology
A2626	Ependymal tumor/anaplastic ependymoma grade III	Supratentorial ependymoma, subtype ZFTA-RELA fused, subclass A	Tumor type is consistent; subtypes are represented in more detail on WHO 2021 but do not include anaplastic ependymoma	Concordant with histology; fusion confirmed by RNA-seq
C2592	Other astrocytic/pilocytic astrocytoma grade I	Pilocytic astrocytoma, infratentorial	Subtype pilocytic astrocytoma of the type circumscribed astrocytic gliomas	Concordant with histology
A2884	Other astrocytic/pilocytic astrocytoma grade I	Pilocytic astrocytoma, infratentorial	Subtype pilocytic astrocytoma of the type circumscribed astrocytic gliomas	Concordant with histology
A8382	Other/differential diagnosis includes high-grade astrocytic/pilocytic xanthoastrocytoma	Atypical malignant peripheral nerve sheath tumor	Subtype malignant peripheral nerve sheath tumor of the type cranial and paraspinal nerve tumors	Difficult diagnosis; NF2 mutation*

Classification of nine tumors on 12.5 that previously yielded scores ≤ 0.30 on 11b4. Two additional tumors within this score category, A9145 and C4495, showed discordance between histologic and methylation-based diagnoses and are represented in Table 7. Germinomas ($n = 2$) are not included in the table as they were not able to be classified on 11b4. Tumor A8382 classified to a type distinct from histology; however, it was diagnostically challenging, and it was not counted as being discordant. Two tumors, C2073 and A4751, classified to new subgroups represented in WHO 2021 and not 2016 (C2073) and to a new entity described in 12.5 and in a recent update of WHO 2021¹⁸ (A4751) and were not considered discordant.

NF2, NM_000268: c.551G>A, p.(Trp184) (National Center for Biotechnology Information GenBank, <https://www.ncbi.nlm.nih.gov/genbank>, last accessed May 23, 2023), detected consistent with classification.

NOS, not otherwise specified; RNA-seq, RNA sequencing; WHO, World Health Organization.

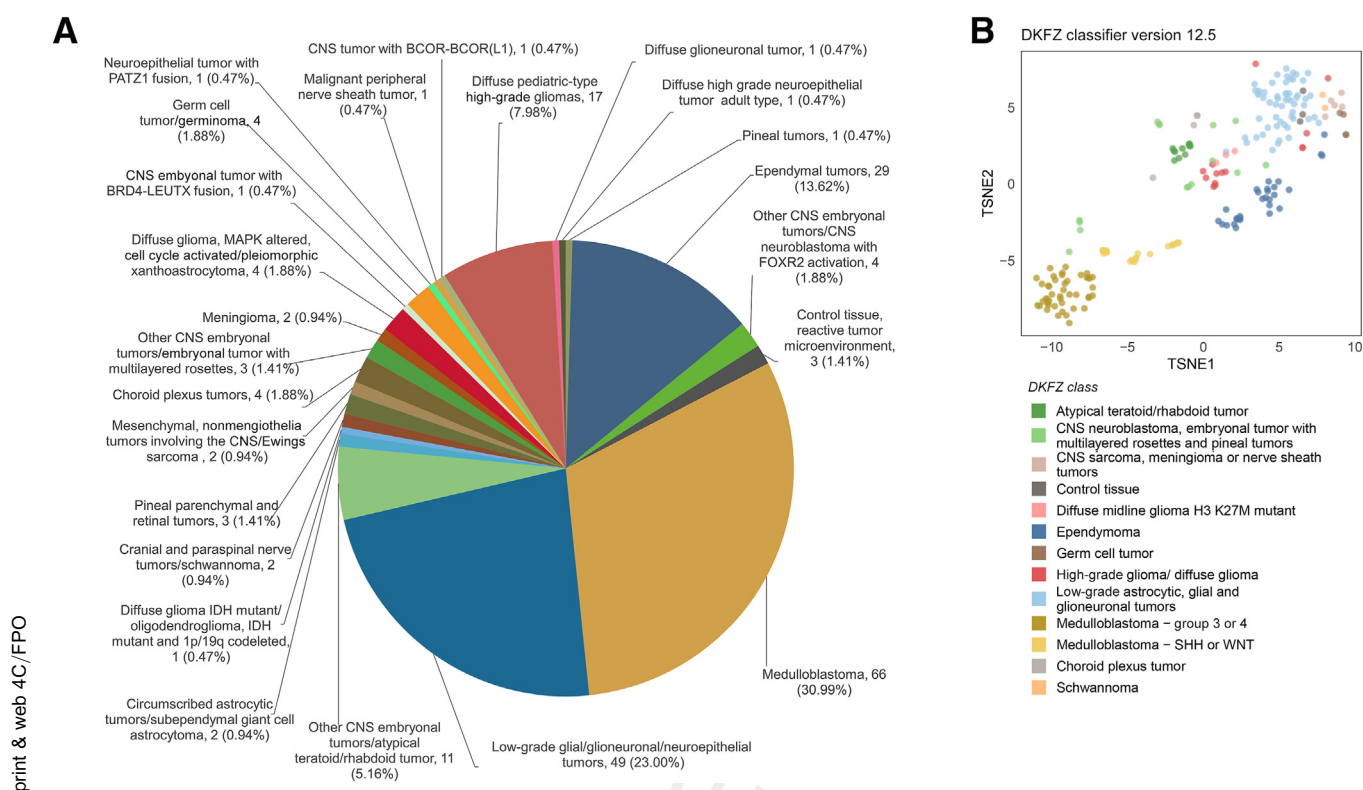


Figure 4 Version 12.5 tumor classifications with scores ≥ 0.90 . Classification scores ≥ 0.90 were obtained for 213 tumors on classifier 12.5. **A:** Most of these samples classified as medulloblastomas, low-grade gliomas, or ependymal tumors; however, high- and low-grade gliomas were better represented than on 11b4. **B:** t-SNE analysis of 213 tumors showed clustering of related tumors according to their overall class. Subclass detail is not shown for all tumors. CNS, central nervous system; DKFZ, Deutsches Krebsforschungszentrum (German Cancer Research Center); MAPK, mitogen-activated protein kinase.

12.5. These tumors included two germinomas, a group not represented on classifier 11b4. The remaining 11 tumors reclassifying ≥ 0.90 are shown in Tables 7 ($n = 2$) and 9 ($n = 9$) and include pilocytic astrocytomas but also some rare gene fusion subgroups. Of the tumors in Table 9 reclassifying ≥ 0.90 , C2073 and A2626 had *MNI-PATZ1* and *ZFTA-RELA* fusions confirmed by sequencing, supporting the respective methylation classifications as neuroepithelial tumor with *MNI-PATZ1* fusion and supratentorial ependymoma, subtype *ZFTA-RELA* fused, subclass A. Tumor A8382 had an *NF2* mutation, *NF2*, NM_000268.4: c.551G>A, p.(Trp184*) (NCBI GenBank, <https://www.ncbi.nlm.nih.gov/genbank>, last accessed May 23, 2023), which is consistent with its classification as an atypical peripheral nerve sheath tumor.

Classification Scores on Classifier Version 12.5 and Tumor Content

Re-evaluation of tumors on classifier version 12.5 did not reveal significant differences in tumor content between tumor groups classifying >0.90 and <0.90 . Half of the 66 tumors (64 plus two germinomas) that fell within the range 0.31 to 0.89 on classifier 11b4 were classified ≥ 0.90 [$n = 33$ (50%)]. These classifications included three samples classified as control tissue, reactive tumor

microenvironment. The remaining 33 tumors were below the 0.90 threshold, with 25 in the range 0.31 to 0.89 and 8 scoring <0.31 . Of the 33 tumors reclassifying ≥ 0.90 , the average tumor content was $65.2\% \pm 21\%$. In tumors with scores from 0.31 to 0.89, it was $64\% \pm 21\%$; and in tumors with scores of <0.30 , it was $62\% \pm 30\%$. As the mean tumor content in all three groups was similar, there is no clear association between sample tumor content and classification scores.

Discussion

Our study is one of the first prospective trials examining the diagnostic utility of DNA methylation array profiling for CNS tumors in a pediatric population and ran in parallel with MNP2.0. Notably, it is the first to report on a large interlaboratory comparative data set to provide a comprehensive picture of test reproducibility in different laboratory settings.

Capper et al,⁵ in the first comprehensive report of CNS tumor methylation profiling using DNA methylation arrays, reported 88% with scores >0.90 in a combined population of adult and pediatric tumors. A total of 14.2% had a diagnosis based on methylation profiling that did not initially match histopathology; however, on re-evaluation, a greater concordance was achieved. Capper et al⁵ also

using the recently released version 12.5 of the classifier improved the diagnostic yield in our study to 79%. Significantly, classifier 12.5 improved the classification of both high- and low-grade gliomas as well as refined subgroup classifications for these groups and for ependymal tumors. A small number of classification score discrepancies was noted between classifier versions 11b4 and 12.5 (5%); however, only 1 of 269 (0.4%) gave a discrepant classification with a high confidence classification score.

A small number of cases in our study with mismatched histopathology and methylation classification had molecular tumor board review, and in two of three cases, the final diagnosis favored tumor histopathology rather than the methylation classification. Although histopathology is fundamental, methylome testing is now recommended for diagnostic guidance in WHO 2021 for several pediatric tumor categories, including high-grade glioma, high-grade astrocytoma, diffuse glioneuronal tumors, posterior fossa ependymoma, SHH-activated medulloblastoma, and non-WNT/non-SHH medulloblastoma.³ In addition, clinical trials are beginning where exclusion criteria specify methylation-based confirmation of tumor subtype, particularly in the context of medulloblastoma. One example is PBTC-053: A Pediatric Brain Tumor Consortium Phase I/II and Surgical Study of CX-4945 in Patients with Recurrent SHH Medulloblastoma (NCT03904862, <https://clinicaltrials.gov>, last accessed February 21, 2023).

It was clear from our analysis that the tumor composition of the test cohort influences the diagnostic yield, with a high proportion of medulloblastoma, ependymoma, or atypical teratoid/rhabdoid tumors, which represented 56% of the total cohort, leading to a bias toward higher classification scores and greater test utility using classifier 11b4. This is likely a consequence of more refined molecular subgroup characterization in the former tumors compared with the gliomas, or it may reflect other issues, such as tumor heterogeneity, and differences in resection and sampling. Tumor content can also affect the test diagnostic yield. Although some previous studies test specimens with an approximate tumor content of 70%, we requested specimens for testing with tumor content of >50%. For several specimens tested, the tumor content was not stated or was below the 50% threshold; however, these tumors were not excluded, and in many instances generated diagnostically relevant classifier scores. In our validation cohort, the assigned tumor content threshold of >50% also did not lead to statistically significant differences in classification score outcomes compared with testing in the DKFZ reference laboratory. Furthermore, tumor content did not appear to significantly impact scores on classifier 12.5, and we conclude that a tumor content in specimens of at least 50% is probably adequate. Also, in our experience, as a general rule, array data should cluster close to the baseline, with variation from this indicative only of copy number changes or locus-specific amplifications or deletions that also show tight data point clustering. Tight array data with a low classification score and CpG count of greater than

approximately 835,000, however, may be indicative of a rare tumor that is not yet represented on the classifier or, potentially, a sample where a definitive classification cannot be made because of contamination with normal tissue or extensive tumor heterogeneity.

Overall concordance between WHO 2016 group histopathology and methylation group classification was evident in 93% of cases in our study when classifications ≥ 0.90 on 11b4 were considered (or 88% of cases when assessed at the WHO 2016 group histology and methylation subgroup level). In more than half of these cases, molecular subgroup information was obtained by applying methylation profiling. This information would normally otherwise be obtained by sequencing, cytogenomics, or immunohistochemistry at increased cost to diagnostics process. For 60 tumors in our test cohort, additional molecular information was available at diagnosis from histopathology, cytogenomics, and sequencing that pointed to a diagnostic subgroup. Of 31 medulloblastomas with a subgroup classification determined by immunohistochemistry, fluorescence *in situ* hybridization, cytogenetics, or single-nucleotide polymorphism microarray, 100% were in agreement with their methylation classification. Eight ependymomas subgrouped by immunohistochemistry and molecular cytogenetics were in 100% agreement with methylation classifications, and 100% of pilocytic astrocytomas classified concordantly as being either midline or of the posterior fossa ($n = 16$). Other tumors with concordant histology, molecular analysis, and immunohistochemistry with methylation array results in this series included one embryonal tumor with multilayered rosettes, one pleomorphic xanthoastrocytoma, one Ewing tumor, one dysembryoplastic neuroepithelial tumor, and one ganglioglioma. This analysis demonstrates the reliability of the classifier version 11b4 to correctly assign tumor subgroups and reinforces the utility and potential of the platform in brain tumor diagnostics in minimizing additional testing.

Capper et al⁵ described a validation cohort of 53 cases tested on Illumina 450 K arrays in their supplementary information, with two discordant classifications giving an overall classification concordance of 96% (51/53). We achieved comparable results on a larger prospective validation cohort on the EPIC 850 K bead chip (103 cases) with concordant classification scores (≥ 0.90) in 93% (75/81) of cases and concordant methylation group and subgroup classifications in 100% of these cases. Intralaboratory variation was also minimal, attesting to the robust nature of the test platform.

In summary, we demonstrated that methylation profiling is a reproducible, sensitive, and reliable platform with great utility for facilitating the classification of pediatric CNS tumors. For brain tumors where histopathology classifications can be ambiguous, including ependymomas and choroid plexus tumors,¹⁹ for medulloblastomas where the addition of molecular subgroups with clinical staging has clear benefits when compared with clinical staging alone for risk stratification,²⁰ and for subclassification of pediatric

glioblastoma, methylation profiling is a valuable diagnostic platform involving a single assay. As we wanted to compare the performance of the platform to previous published studies that have used classifier versions 11b2-4 exclusively, we have presented data for both classifiers 11b4 and 12.5. There are currently little published data available for classifier 12.5. In conclusion, the methylation workflow is straightforward, with extensive data generated from a single test platform, and is likely to become an invaluable adjunct to histopathology in the near future.

Acknowledgments

We thank all the patients and their families for participation; the Monash Health Translation Precinct Medical Genomics Core Facility for support; and Duncan MacGregor for review of difficult cases.

Author Contributions

C.L.W. performed data acquisition (laboratory processing and data entry and analysis), curation (study database review and data extraction), analysis (review of laboratory data), interpretation (integration of clinical and laboratory data), and manuscript drafting and editing; K.M.K. performed data acquisition (data entry and database maintenance), curation (study database review and data extraction), and manuscript editing and review; M.K.B. performed data acquisition (laboratory processing and data entry and analysis) and manuscript review; E.R. performed data acquisition (laboratory processing and data entry and analysis) and manuscript review; R.S. obtained resources [AIM BRAIN (AB) grant funding and study sponsorship] and performed conceptualization [study design and AB/Molecular Neuro-pathology 2.0 (MNP2.0) integration] and manuscript review; J.M.J. obtained resources (AB grant funding and study sponsorship) and performed conceptualization (study design and AB/MNP2.0 integration) and manuscript review; J.E.C. obtained resources and performed data review and manuscript review; D.S. obtained resources (MNP2.0 grant funding and study sponsorship) and performed data acquisition (MNP2.0 laboratory data analysis), conceptualization (MNP2.0 study design and AB/MNP2.0 integration), and manuscript review; F.S. obtained resources (MNP2.0 grant funding and study sponsorship) and performed data acquisition (MNP2.0 laboratory data analysis), conceptualization (MNP2.0 study design and AB/MNP2.0 integration), and manuscript review; D.T.W.J. obtained resources (MNP2.0 grant funding and study sponsorship) and performed conceptualization and manuscript review; S.M.P. obtained resources (MNP2.0 grant funding and study sponsorship) and performed conceptualization and manuscript review; T.R. performed data acquisition (local histology analysis and tumor board review) and manuscript review; C.D.'A. performed data acquisition (local histology analysis and

tumor board review) and manuscript review; M.L.R. performed data acquisition (local histology analysis and tumor board review) and manuscript review; J.M.D. performed data acquisition (local histology analysis and tumor board review) and manuscript review; R.J. performed data acquisition (local histology analysis and tumor board review) and manuscript review; D.D.B. performed visual formatting of data and manuscript review; M.J.D. performed visual formatting of data and manuscript review; P.W. performed data acquisition (patient recruitment and clinical data provision) and manuscript review; T.H. performed data acquisition (patient recruitment and clinical data provision) and manuscript review; D.S.Z. performed data acquisition (patient recruitment and clinical data provision) and manuscript review; S.K. performed data acquisition (patient recruitment and clinical data provision) and manuscript review; G.M. performed data acquisition (patient recruitment and clinical data provision) and manuscript review; F.A. performed data acquisition (patient recruitment and clinical data provision) and manuscript review; M.K. performed data acquisition (patient recruitment and clinical data provision) and manuscript review; J.A.H. performed data acquisition (patient recruitment and clinical data provision) and manuscript review; K.T. performed data acquisition (patient recruitment and clinical data provision) and manuscript review; A.D. performed data acquisition (patient recruitment and clinical data provision) and manuscript review; D.D.E. performed data acquisition (patient recruitment and clinical data provision) and manuscript review; D.-A.K.-Q. performed data acquisition (patient recruitment and clinical data provision) and manuscript review; M.W. obtained resources (AB grant funding) and performed data acquisition (laboratory data review), analysis (laboratory data review), interpretation (integration of clinical and laboratory data), and manuscript review; E.M.A. obtained resources (AB grant funding) and performed conceptualization (study design and AB/MNP2.0 integration), data acquisition (laboratory data review), curation (study database review and data extraction), analysis (review of laboratory data), interpretation (integration of clinical and laboratory data), and manuscript drafting and editing; N.G.G. obtained resources (AB grant funding) and performed conceptualization (study design and AB/MNP2.0 integration), data acquisition (patient recruitment and clinical data provision), interpretation (integration of clinical and laboratory data), and manuscript editing and review; and J.R.H. obtained resources (AB grant funding) and performed conceptualization (study design and AB/MNP2.0 integration), data acquisition (patient recruitment and clinical data provision), interpretation (integration of clinical and laboratory data), and manuscript editing and review.

Supplemental Data

Supplemental material for this article can be found at <http://10.1016/j.jmoldx.2023.06.013>.

References

1. Louis DN, Perry A, Reifenberger G, von Deimling A, Figarella-Branger D, Cavenee WK, Ohgaki H, Wiestler OD, Kleihues P, Ellison DW: The 2016 World Health Organization classification of tumors of the central nervous system: a summary. *Acta Neuropathol* 2016, 131:803–820
2. Louis DN, Perry A, Burger P, Ellison DW, Reifenberger G, von Deimling A, Aldape K, Brat D, Collins VP, Eberhart C, Figarella-Branger D, Fuller GN, Giangaspero F, Giannini C, Hawkins C, Kleihues P, Korshunov A, Kros JM, Beatriz Lopes M, Ng HK, Ohgaki H, Paulus W, Pietsch T, Rosenblum M, Rushing E, Soylemezoglu F, Wiestler O, Wesseling P, International Society Of N-H: International Society of Neuropathology–haarlem consensus guidelines for nervous system tumor classification and grading. *Brain Pathol* 2014, 24:429–435
3. Louis DN, Perry A, Wesseling P, Brat DJ, Cree IA, Figarella-Branger D, Hawkins C, Ng HK, Pfister SM, Reifenberger G, Soffiatti R, von Deimling A, Ellison DW: The 2021 WHO classification of tumors of the central nervous system: a summary. *Neuro Oncol* 2021, 23:1231–1251
4. Louis DN, Wesseling P, Aldape K, Brat DJ, Capper D, Cree IA, et al: cIMPACT-NOW update 6: new entity and diagnostic principle recommendations of the cIMPACT-Utrecht meeting on future CNS tumor classification and grading. *Brain Pathol* 2020, 30:844–856
5. Capper D, Jones DTW, Sill M, Hovestadt V, Schrimpf D, Sturm D, et al: DNA methylation-based classification of central nervous system tumours. *Nature* 2018, 555:469
6. Capper D, Stichel D, Sahm F, Jones DTW, Schrimpf D, Sill M, Schmid S, Hovestadt V, Reuss DE, Koelsche C, Reinhardt A, Wefers AK, Huang K, Sievers P, Ebrahimi A, Scholer A, Teichmann D, Koch A, Hanggi D, Unterberg A, Platten M, Wick W, Witt O, Milde T, Korshunov A, Pfister SM, von Deimling A: Practical implementation of DNA methylation and copy-number-based CNS tumor diagnostics: the Heidelberg experience. *Acta Neuropathol* 2018, 136:181–210
7. Pickles JC, Fairchild AR, Stone TJ, Brownlee L, Merve A, Yasin SA, et al: DNA methylation-based profiling for paediatric CNS tumour diagnosis and treatment: a population-based study. *Lancet Child Adolesc Health* 2020, 4:121–130
8. Jaunmuktane Z, Capper D, Jones DTW, Schrimpf D, Sill M, Dutt M, Suraweera N, Pfister SM, von Deimling A, Brandner S: Methylation array profiling of adult brain tumours: diagnostic outcomes in a large, single centre. *Acta Neuropathol Commun* 2019, 7:24
9. Priesterbach-Ackley LP, Boldt HB, Petersen JK, Bervoets N, Scheie D, Ulhoi BP, Gardberg M, Brannstrom T, Torp SH, Aronica E, Kusters B, den Dunnen WFA, de Vos F, Wesseling P, de Leng WWJ, Kristensen BW: Brain tumour diagnostics using a DNA methylation-based classifier as a diagnostic support tool. *Neuropathol Appl Neurobiol* 2020, 46:478–492
10. Karimi S, Zuccato JA, Mamatjan Y, Mansouri S, Suppiah S, Nassiri F, Diamandis P, Munoz DG, Aldape KD, Zadeh G: The central nervous system tumor methylation classifier changes neuro-oncology practice for challenging brain tumor diagnoses and directly impacts patient care. *Clin Epigenetics* 2019, 11:185
11. Hovestadt V, Remke M, Kool M, Pietsch T, Northcott PA, Fischer R, Cavalli FM, Ramaswamy V, Zapatka M, Reifenberger G, Rutkowski S, Schick M, Bewerunge-Hudler M, Korshunov A, Lichter P, Taylor MD, Pfister SM, Jones DT: Robust molecular sub-grouping and copy-number profiling of medulloblastoma from small amounts of archival tumour material using high-density DNA methylation arrays. *Acta Neuropathol* 2013, 125:913–916
12. Esteller M, Garcia-Foncillas J, Andion E, Goodman SN, Hidalgo OF, Vanaclocha V, Baylin SB, Herman JG: Inactivation of the DNA-repair gene MGMT and the clinical response of gliomas to alkylating agents. *N Engl J Med* 2000, 343:1350–1354
13. Christians A, Hartmann C, Benner A, Meyer J, von Deimling A, Weller M, Wick W, Weiler M: Prognostic value of three different methods of MGMT promoter methylation analysis in a prospective trial on newly diagnosed glioblastoma. *PLoS One* 2012, 7:e33449
14. Northcott PA, Buchhalter I, Morrissy AS, Hovestadt V, Weischenfeldt J, Ehrenberger T, et al: The whole-genome landscape of medulloblastoma subtypes. *Nature* 2017, 547:311–317
15. Sturm D, Capper D, Andreiulo F, Gessi M, Kolsche C, Reinhardt A, et al: Multiomic neuropathology improves diagnostic accuracy in pediatric neuro-oncology. *Nat Med* 2023, 29:917–926
16. R Core Team: R: A Language and Environment for Statistical Computing. Vienna, Austria, R Foundation for Statistical Computing, 2018
17. Northcott PA, Shih DJ, Peacock J, Garzia L, Morrissy AS, Zichner T, et al: Subgroup-specific structural variation across 1,000 medulloblastoma genomes. *Nature* 2012, 488:49–56
18. Komori T: Update of the 2021 WHO classification of tumors of the central nervous system: adult diffuse gliomas. *Brain Tumor Pathol* 2023, 40:1–3
19. Ellison DW, Kocak M, Figarella-Branger D, Felice G, Catherine G, Pietsch T, Frappaz D, Massimino M, Grill J, Boyett JM, Grundy RG: Histopathological grading of pediatric ependymoma: reproducibility and clinical relevance in European trial cohorts. *J Negat Results Biomed* 2011, 10:7
20. Pfister S, Hartmann C, Korshunov A: Histology and molecular pathology of pediatric brain tumors. *J Child Neurol* 2009, 24:1375–1386